Title

State-Dependent Functional Dysconnectivity in Youth With Psychosis Spectrum Symptoms

Journal

Schizophrenia Bulletin, 46(2)

ISSN

0586-7614

Authors

Mennigen, Eva
Jolles, Dietsje D
Hegarty, Catherine E
et al.

Publication Date

2020-02-26

DOI

10.1093/schbul/sbz052

Schizophrenia Bulletin vol. 46 no. 2 pp. 408–421, 2020
doi:10.1093/schbul/sbz052
Advance Access publication 20 June 2019

State-Dependent Functional Dysconnectivity in Youth With Psychosis Spectrum Symptoms

Eva Mennigen[1], Dietsje D. Jolles[2], Catherine E. Hegarty[2], Mohan Gupta[2], Maria Jalbrzikowski[3], Loes M. Olde Loohuis[4], Roel A. Ophoff[1,4], Katherine H. Karlsgodt[1,2], and Carrie E. Bearden*[,1,2]

[1]Department of Psychiatry and Biobehavioral Sciences, Semel Institute for Neuroscience and Human Behavior, University of California, Los Angeles, Los Angeles, CA; [2]Department of Psychology, University of California, Los Angeles, Los Angeles, CA; [3]Department of Psychiatry, University of Pittsburgh, Pittsburgh, PA; [4]Center for Neurobehavioral Genetics, University of California, Los Angeles, Los Angeles, CA

*To whom correspondence should be addressed; tel: +1 310 825 3458, fax: +1 310 825 6766, e-mail: cbearden@mednet.ucla.edu

Psychosis spectrum disorders are conceptualized as neurodevelopmental disorders accompanied by disruption of large-scale functional brain networks. Dynamic functional dysconnectivity has been described in patients with schizophrenia and in help-seeking individuals at clinical high risk for psychosis. Less is known, about developmental aspects of dynamic functional network connectivity (dFNC) associated with psychotic symptoms (PS) in the general population. Here, we investigate resting state functional magnetic resonance imaging data using established dFNC methods in the Philadelphia Neurodevelopmental Cohort (ages 8–22 years), including 129 participants experiencing PS and 452 participants without PS (non-PS). Functional networks were identified using group spatial independent component analysis. A sliding window approach and k-means clustering were applied to covariance matrices of all functional networks to identify recurring whole-brain connectivity states. PS-associated dysconnectivity of default mode, salience, and executive networks occurred only in a few states, whereas dysconnectivity in the sensorimotor and visual systems in PS youth was more pervasive, observed across multiple states. This study provides new evidence that disruptions of dFNC are present even at the less severe end of the psychosis continuum in youth, complementing previous work on help-seeking and clinically diagnosed cohorts that represent the more severe end of this spectrum.

Key words: dynamic functional network connectivity/psychosis spectrum/independent component analysis/adolescence

Introduction

Substantial evidence now indicates that psychotic symptoms (PS) occur on a continuum ranging from subthreshold PS to full-blown psychotic disorders such as schizophrenia.[1–3] Traditionally, individuals on the severe end of this continuum have been studied. But more recently, there has been increasing interest in individuals experiencing a broader spectrum of PS. First, because they are at increased risk of progressing to overt illness,[4,5] but second because they offer the opportunity to explore neural changes in the absence of confounds from medication or disease chronicity.

The psychosis continuum is considered to have neurodevelopmental underpinnings concomitant with altered brain and cognitive maturation.[6–10] Symptoms of many psychiatric illnesses appear during adolescence, a sensitive period of brain development,[11–13] and frequency of PS peaks in adolescence.[2,14] Therefore, brain imaging studies of youth experiencing PS are likely to be informative regarding neural substrates of developmental vulnerability to psychosis. Publicly available data from the Philadelphia Neurodevelopmental Cohort (PNC) used in this study offer an unprecedented opportunity to study neural substrates of PS from late-childhood through adolescence and early adulthood, overlapping with critical periods for the onset of many neuropsychiatric disorders.[15,16]

There is now a wealth of evidence that disruption of large-scale synchronized neural connectivity plays a role in the pathophysiology of schizophrenia.[17–19] Functional connectivity describes the correlated temporal fluctuations of distant brain areas and is often assessed during resting state functional magnetic resonance imaging (rs-fMRI) while participants are not engaged in a particular task.[20–22] In terms of static functional connectivity, which reflects the averaged connectivity across the entire resting state scan, previous findings in PS youth in this cohort include *hyper*connectivity within the default

mode network (DMN) that was associated with poorer cognitive performance, and *hypo*connectivity within the cognitive control (CC) domain.[9,23–25] These patterns resemble those observed in patients with overt schizophrenia and in help-seeking individuals at clinical high risk (CHR) for psychosis.

Recently, has it emerged that functional connectivity is a dynamic process that exhibits considerable fluctuations across the duration of a typical resting state scan.[23,24,26] Greater variability in network activity is associated with increased capacity for information processing,[25] and thus may index better overall "brain health".[27,28] With the emergence of new methods, we are now poised to explore the dynamics of functional dysconnectivity related to PS.[23,29–32]

Recently, we investigated dynamic functional network connectivity (dFNC) using a sliding window approach[29] to identify recurring whole-brain connectivity patterns in treatment-seeking CHR individuals.[33] Overall fluctuations of connectivity across dynamic states in CHR individuals were reduced relative to healthy controls. Further, CHR individuals exhibited qualitatively similar, but milder, dysconnectivity relative to patients with schizophrenia.[34] Applying a different approach to capture dynamics of functional connectivity,[31] Barber et al[35] investigated healthy adults who self-reported psychotic-like experiences; individuals reporting these symptoms spent more time in states that showed intra-DMN hypoconnectivity, consistent with findings in patients with overt schizophrenia.[36,37]

This emerging literature suggests that naturally occurring functional connectivity changes are aberrant in schizophrenia and across the broader psychosis spectrum. Frequently observed dysconnectivity between CC and DMN domains may occur only in certain dFNC states. Further, both individuals with overt schizophrenia and healthy adults endorsing psychotic-like experiences exhibited longer dwell times in brain states characterized by intra-DMN hypoconnectivity.

We hypothesize that youth experiencing PS will exhibit dwell time differences similar to those observed in previous studies of help-seeking CHR individuals, and state-dependent dysconnectivity between DMN and CC domains, further substantiating the notion of a continuum of dysconnectivity associated with PS across the lifespan. Therefore, we investigated whole-brain dFNC and associated summary metrics in PS youth relative to their peers who do not experience PS (non-PS).

Methods

Study Participants

A socioeconomically diverse community sample of nonclinically ascertained participants aged 8–22 years was included in the PNC study. Participants were broadly recruited from the Children's Hospital of Philadelphia.

Study participants ($n = 9428$) completed a computerized structured interview (GOASSESS) that included a psychopathology screening based on the National Institute of Mental Health Genetic Epidemiology Research Branch Kiddie—Schedule for Affective Disorders and Schizophrenia (K-SADS),[38] which provides clinical symptom and episode information[39] (supplementary material 1.1), and a computerized neurocognitive battery.[40] Multimodal MRI was acquired for a subsample of participants ($n = 1445$).[41]

Of 799 participants with rs-fMRI scans, imaging data of 581 participants passed quality control. Demographics are summarized in table 1.

Psychosis Spectrum Classification

We identified PS individuals in the cohort according to criteria introduced by Calkins et al,[43] which have been widely applied in studies on this cohort.[8,9,44–46] Briefly, PS were determined based on the PRIME Screen-Revised[47] assessing positive symptoms, the K-SADS[48] for hallucinations and delusional symptoms, and the Scale of Prodromal Syndromes (SOPS)[49] assessing negative and disorganized symptoms (see supplementary materials 1.2 and 1.3).

Resting State fMRI Data and Preprocessing

Eyes-open rs-fMRI data were collected on a single scanner with 3T field strength over 6.2 min. FMRIB Software Library (https://fsl.fmrib.ox.ac.uk/fsl) and Analysis of Functional NeuroImages (https://afni.nimh.nih.gov) tools were used for functional preprocessing that included slice time correction, motion correction, grand mean scaling, and smoothing (6 mm kernel; see supplementary material 1.4).

Group Independent Component Analysis

RS-fMRI data were decomposed into 100 components using group-level spatial independent component analysis (ICA)[50] using the group ICA fMRI toolbox (http://mialab.mrn.org/software/gift).

On the basis of the following criteria, 59 intrinsic connectivity networks (ICNs) were identified:[51] peak activation in gray matter with no or minimal overlap with white matter, ventricles, or non-brain structures and maximal power in lower frequencies (< 0.1 Hz). ICNs were assigned to 9 functional domains based on their anatomical location[52] and prior scientific literature[53]: subcortical, salience, auditory, sensorimotor, visual, CC, DMN, limbic, and cerebellum (figure 1 and supplementary material 1.5).

Dynamic FNC

We applied a sliding temporal window approach to capture changes of whole-brain connectivity (see supplementary

Table 1. Demographics and Motion Parameters

	Non-PS *n* = 452	PS *n* = 129	*P* value
Age (SD)	15.2 (3.20)	15.00 (2.8)	n.s.
Sex (% female)	55.3	56.6	n.s.
Ethnicity (%)			
AA	35.8	57.4	.001
EA	54.2	31.0	
Other	10.0	11.6	
WRAT (raw score)	54.36 (8.6)	51.21 (9.04)	<.05
Education (years)	8.83 (3.2)	8.46 (2.8)	n.s.
Maternal education (years)	14.4 (2.5)	13.8 (2.2)	<.05
PS-R (total score)	3.86 (5.6)	21.59 (13.8)	<.05
SOPS (total score of negative/disorganized symptoms)	1.33 (1.83)	3.98 (4)	<.05
K-SADS (severity of hallucinations/delusions)	0.55 (2.07)	4.9 (5.26)	<.05
Sum of endorsed depressive symptoms	1.34 (1.91)	2.2 (1.76)	<.05
Sum of endorsed manic symptoms	1.5 (2.92)	3.86 (2.97)	<.05
N meeting ADHD criteria (yes:no)*	8	11	<.05
Relative movement (mm)	0.59 (0.29)	0.65 (0.29)	<.05
Maximum movement (mm)	0.7 (0.59)	0.77 (0.57)	n.s.
Spike count	4.38 (5.3)	5.24 (5.6)	n.s.

Note: PS, psychosis spectrum youth; AA, African American; EA, European American; WRAT, wide range achievement test; PS-R, PRIME screen revised; SOPS, scale of prodromal symptoms; K-SADS, Kiddie schedule for affective disorders and schizophrenia; ADHD, attention-deficit/hyperactivity disorder *criteria according to Kessler et al.[42]

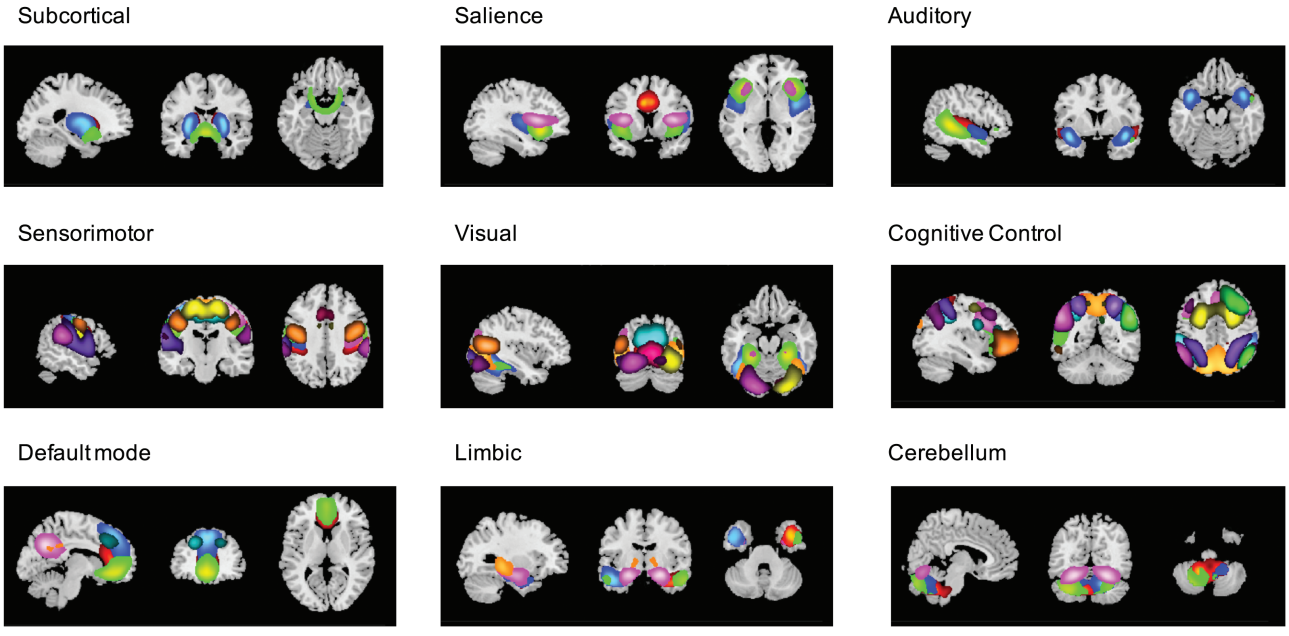

Fig. 1. Functional domains and their assigned intrinsic connectivity networks.

material 1.6).[29] Briefly, a tapered window slides across concatenated time courses and for each window a FNC matrix consisting of ICN-to-ICN Pearson's correlations was calculated.

From each participant, windows with the highest variance in FNC were chosen to initialize clustering. K-means clustering was first performed on the local extrema with varying numbers of clusters *k* (2–20): The ratio of within- to between-cluster distances was plotted for each *k*. The turning point in the graph where the amount of additionally explained variance becomes marginal, and therefore reflecting the optimal number of clusters (elbow criterion), was 5.[54]

These 5 cluster centroids were used as starting points to cluster all windowed FNC matrices in such a way that each windowed FNC matrix was assigned to the one cluster with which it was most highly correlated. For each participant, each dynamic state is represented by

the element-wise median connectivity across all windows assigned to this particular state.

Model Selection

We applied a multivariate backward model selection approach adapted from the MANCOVAN toolbox implemented in GIFT to account for important covariates and to prevent the model from overfitting.[51] Assuming that each dynamic state may be influenced differently by the covariates, statistical models were generated for each state separately. The initial full model for all dynamic states included the following variables: group (non-PS vs PS), sex, age, maternal education, and their interactions (see supplementary material 1.7). As in other studies of this cohort,[14] maternal education was included as a proxy for socioeconomic status.[55]

The following models were selected for the 5 dynamic states:

state 1: FNC ~ (group, sex, age, group × sex) × β + ε
state 2: FNC ~ (sex, age, maternal education) × β + ε
state 3: FNC ~ (group, sex, age, maternal education) × β + ε
state 4: FNC ~ (group, sex, age, maternal education, group × age, sex × maternal education) × β + ε
state 5: FNC ~ (group, sex, age, maternal education, group × maternal education) × β + ε

The reduced models were then used for further univariate tests in which we included the mean frame-wise displacement (FD) to further account for motion.[51] Results were corrected for a false discovery rate (FDR; $q = 0.05$).

For ICN pairs that exhibited a significant group difference, the relationship between dFNC and a continuous symptom measure (ie, sum of PRIME Screen-Revised total score, KSADS severity of hallucinations/delusions, and SOPS disorganized/negative symptom total score) was tested in a linear model, including the same variables as in the state-specific analysis and mean FD (see supplementary material 1.8).

We further tested whether group effects were specific to psychosis spectrum symptoms by additionally including depressive and manic symptom scores as covariates in the state-specific models (see supplementary material 1.9).

Dynamic Indices

Summary metrics reflect the dynamic behavior of FNC across the scan: The mean dwell time (MDT) reflects the average time an individual lingers in one particular state before switching to a different state; the fraction of time (FT) summarizes the time across the entire scan that an individual spends in one particular state.

We applied the same backward model selection procedure as for the dFNC analysis with the same set of covariates. The reduced models for FT and MDT included sex, age, and maternal education but not group. Results were FDR-corrected at $q = 0.05$.

Results

Dynamic FNC

The 5 dynamic states are shown in figure 2. We focus on connectivity differences between groups (PS vs non-PS); this variable was included in the reduced models of states 1, 3, 4, and 5. Results regarding the other covariates are detailed in separate supplementary files.

State 1: DMN-CC Domain-Synchronized State

Across all participants, 17% of all windows were assigned to this state. DMN and CC domains appear synchronized in this state: they show high positive connectivity with each other and form one functional domain. Together, they exhibit negative connectivity with the limbic domain and the cerebellum. Further, state 1 shows anticorrelation between the sensorimotor domain and limbic and cerebellar domains.

In this state, 35 ICN-to-ICN connectivity pairs show a significant group effect (figure 3a; table 2). In general, PS youth exhibit reduced connectivity between the CC domain with salience, auditory, cerebellar, sensorimotor, and subcortical domains, between the sensorimotor domain with visual and subcortical domains, and within the DMN. In contrast, increased inter-domain connectivity in PS relative to non-PS youth is observed between the salience domain and DMN and increased *intra*-domain connectivity within the salience and sensorimotor domains.

State 2: Hyperconnected State Without Subcortical Antagonism

State 2 is characterized by increased intra-domain connectivity, particularly in salience, sensorimotor, and cerebellar domains. The visual domain is anticorrelated with sensorimotor, salience, and subcortical domains. Twenty-two percent of all windowed FNC matrices were assigned to this state.

State 3: DMN-CC Domain-Antagonized State

In this state, each functional domain shows positive intra-domain connectivity with the exception of the visual domain. The DMN exhibits anticorrelation with CC, salience, and sensorimotor domains. Twenty-six percent of windowed FNC matrices were clustered into this pattern.

In state 3, 30 ICN-to-ICN connectivity pairs exhibit significant differences between groups (figure 3b; table 3). PS participants show dysconnectivity relative to non-PS youth between the CC and DMN domains, decreased inter-domain connectivity between the sensorimotor and salience and subcortical domains, between the visual domain and DMN, and between limbic and cerebellar domains. However, PS youth show relatively increased

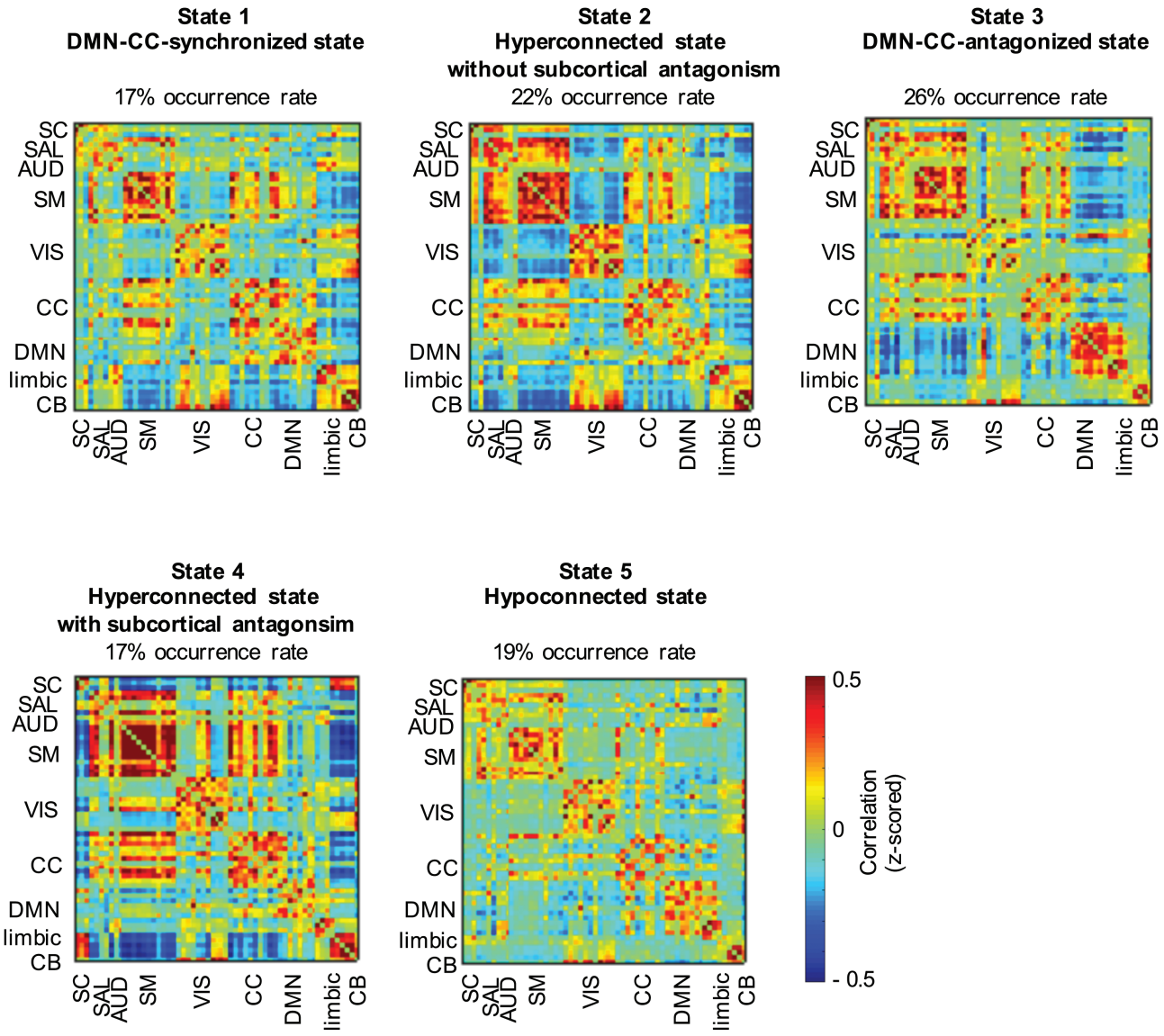

Fig. 2. The 5 dynamic states identified, including their occurrence rates across all participants.

connectivity between the visual and sensorimotor domains and between the DMN and subcortical domains.

State 4: Hyperconnected State With Subcortical Antagonism
State 4 is characterized by increased intra-domain connectivity, particularly within the sensorimotor domain. Negative correlation is observed between the subcortical domain and sensorimotor, CC, and DMN domains, whereas connectivity between subcortical areas and the cerebellum is increased relative to the other states. The overall occurrence rate of this state was 17%.

Two ICN-to-ICN connectivity pairs show a significant group effect (table 4; figure 3c). Here, inter-domain connectivity between visual and CC domains is increased in PS youth relative to non-PS youth. Two ICN pairs also exhibit a significant group by age interaction effect (figure 3e): PS youth exhibit age-associated decreases in connectivity between the right angular gyrus (CC domain) with lingual gyri (visual domain), whereas non-PS participants show no change in connectivity with age. In contrast, connectivity increases with age between the posterior middle temporal gyrus (auditory domain) and the left inferior frontal gyrus (CC domain) in PS but not in non-PS youth (figure 4).

State 5: Globally Hypoconnected State
In this state, connectivity across domains appears diminished and functional domains are less

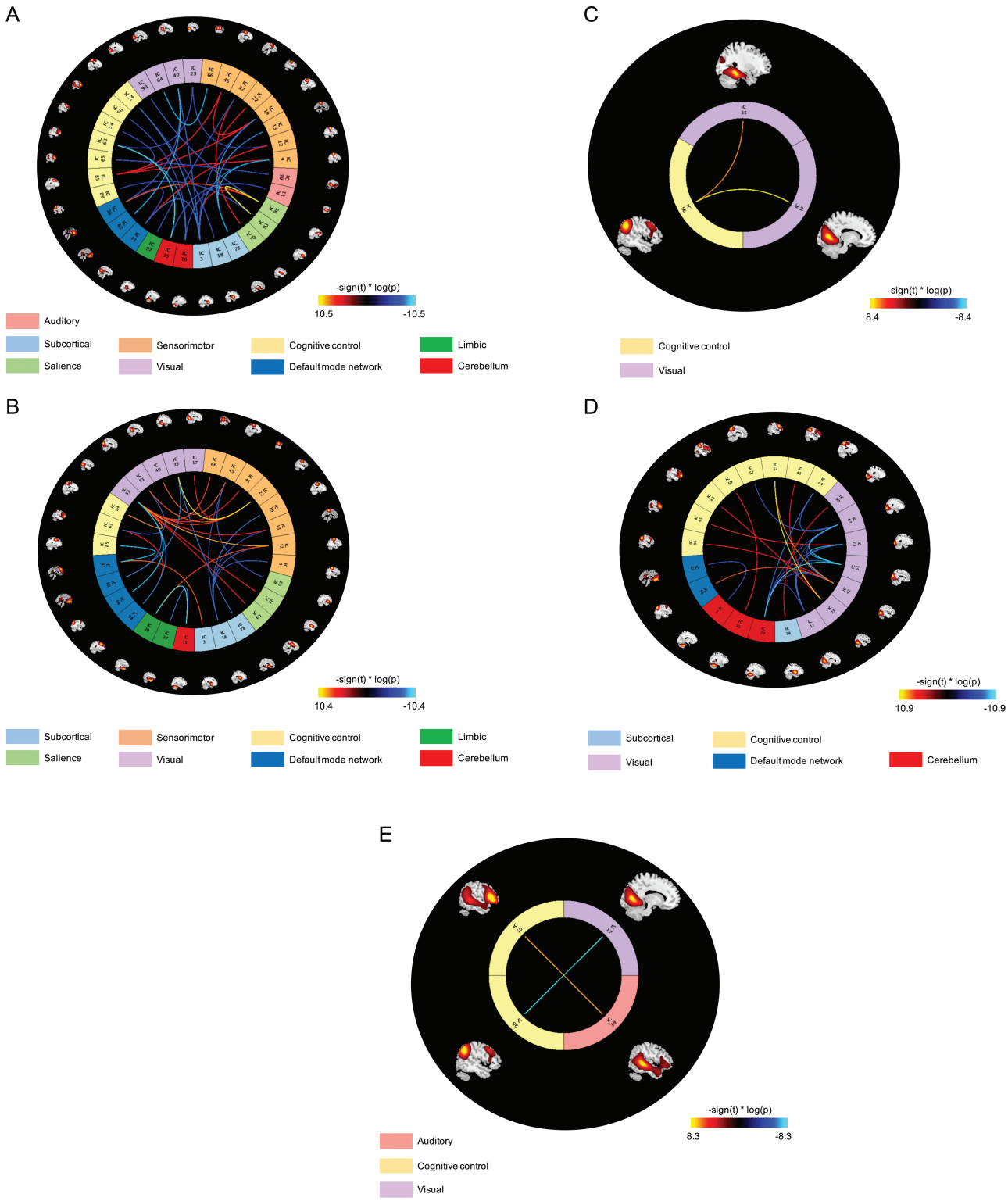

Fig. 3. ICN-to-ICN connections showing significant group effects in (A) state 1, (B) state 3, (C) state 4, and (D) state 5; (E) ICN-to-ICN connections of significant group by age interaction effects in state 4. The scaling, –sign(t) * log(p), provides information on the effect size and direction. The cool color scale represents negative values, indicating hypoconnectivity (decreased positive correlation, or greater anti-correlation) in psychotic symptoms (PS) relative to non-PS youth; the hot color scale represents positive values indicating hyperconnectivity (increased positive correlation or less anti-correlation) in PS relative to non-PS youth. ICN = intrinsic connectivity network.

Table 2. ICN-to-ICN Connectivity Pairs That Show Significant Group Effects in State 1 (DMN-CC-Synchronized State), Ordered by Domains

ICN1	ICN2	Domains	*P* value	*t*-value	Mean connectivity		Relationship
					Non-PS	PS	
Superior temporal gyrus R + L	Cerebellum R + L	AUD-CB	.00145	–3.21	0.01	–.05	PS < non-PS
Superior temporal gyrus R + L	Cerebellum R + L	AUD-CB	.00148	–3.20	–0.02	–0.10	PS < non-PS
Posterior middle temporal Gyrus R + L	Inferior frontal gyrus R	AUD-CC	.00145	–3.20	0.19	0.17	PS < non-PS
Inferior frontal gyrus L	Cerebellum R + L	CC-CB	.00146	–3.20	–0.07	–0.12	PS < non-PS
Frontal pole L	Cerebellum R + L	CC-CB	.00003	–4.23	0.04	–0.06	PS < non-PS
Frontal pole L	Cerebellum R + L	CC-CB	.00037	–3.59	0.01	–0.04	PS < non-PS
Middle frontal gyrus R + L	Superior frontal gyrus	CC-CC	.00254	–3.04	0.33	0.25	PS < non-PS
rACC	Precuneus	DMN-DMN	.00181	–3.14	0.09	0.02	PS < non-PS
Anterior insula R + L	IPL and MFG	SAL-CC	.00268	–3.02	0.01	–0.06	PS < non-PS
Anterior insula R + L	rACC	SAL-DMN	.00040	3.57	0.02	0.10	PS > non-PS
Anterior insula R + L	Anterior insula R + L	SAL-SAL	.00004	4.14	0.21	0.28	PS > non-PS
Insular cortex R + L	preSMA	SAL-SM	.00162	3.17	–0.05	0.03	PS > non-PS
Anterior insula R + L	Lingual gyrus R + L	SAL-VIS	.00056	–3.48	0.02	–0.03	PS < non-PS
Putamen R + L	Superior parietal lobule R+L	SC-CC	.00266	–3.02	–0.03	–0.08	PS < non-PS
Putamen R + L	Precuneus	SC-DMN	.00073	–3.40	–0.10	–0.13	PS < non-PS
Putamen R + L	Anterior insula R + L	SC-SAL	.00230	3.07	0.17	0.22	PS > non-PS
Putamen R + L	Postcentral gyrus L	SC-SM	.00034	–3.61	–0.10	–0.14	PS < non-PS
Putamen R + L	Precentral gyrus R + L	SC-SM	.00261	–3.03	–0.06	–0.10	PS < non-PS
Putamen R + L	Superior parietal lobule R + L	SC-SM	.00032	–3.63	–0.10	–0.15	PS < non-PS
Ventral striatum	Postcentral gyrus L	SC-SM	.00016	–3.80	–0.18	–0.22	PS < non-PS
Ventral striatum	Paracentral lobule medial	SC-SM	.00037	–3.59	–0.18	–0.23	PS < non-PS
Ventral striatum	Precentral gyrus R + L	SC-SM	.00026	–3.69	–0.18	–0.25	PS < non-PS
Putamen R + L	Precuneus	SC-VIS	.00066	–3.43	–0.07	–0.10	PS < non-PS
Postcentral gyrus L	Superior frontal gyrus	SM-CC	.00272	3.01	0.30	0.35	PS > non-PS
Precentral gyrus R + L	Superior frontal gyrus	SM-CC	.00225	3.07	0.28	0.36	PS > non-PS
SMA	Superior frontal gyrus	SM-CC	.00226	3.07	0.42	0.47	PS > non-PS
Postcentral gyrus L	Precuneus	SM-DMN	.00121	3.26	0.02	0.10	PS > non-PS
preSMA	Posterior hippocampus R + L	SM-limbic	.00118	–3.27	–0.18	–0.25	PS < non-PS
Precentral gyrus R + L	Precentral gyrus R + L	SM-SM	.00227	3.07	0.30	0.38	PS > non-PS
Precentral gyrus R + L	SMA	SM-SM	.00172	3.16	0.48	0.57	PS > non-PS
Postcentral gyrus L	Fusiform gyrus R + L	SM-VIS	.00140	–3.21	–0.15	–0.22	PS < non-PS
Supramarginal gyrus R + L	Inferior occipital gyrus R + L	SM-VIS	.00018	–3.78	–0.03	–0.10	PS < non-PS
Fusiform gyrus R + L	Frontal pole L	VIS-CC	.00249	–3.04	0.07	0.01	PS < non-PS
Precuneus	rACC	VIS-DMN	.00116	–3.27	0.06	0.00	PS < non-PS
Precuneus	rACC	VIS-DMN	.00018	–3.78	0.24	0.13	PS < non-PS

Note: ICN, intrinsic connectivity network; PS, participants with psychosis spectrum symptoms; non-PS, participants without psychosis spectrum symptoms; R, right; L, left; CC, cognitive control domain; CB, cerebellum; DMN, default mode network; SAL, salience domain; SM, sensorimotor domain; VIS, visual domain; preSMA, presupplementary motor area; SMA, supplementary motor area; rACC, rostral anterior cingulate cortex.

distinguishable based on their intra-domain connectivity. Of all windowed FNC matrices, 19% were assigned to this state.

In state 5, 25 ICN-to-ICN connectivity pairs show significant differences between non-PS and PS groups (table 5; figure 3d). In particular, connectivity within the visual domain is reduced in PS, whereas connectivity between visual and CC domains is generally increased in PS relative to non-PS youth.

Secondary dFNC Analyses

Psychotic Symptoms as a Continuous Variable

Most ICN pairs that show state-specific group differences also exhibit a significant association with a continuous measure of severity of PS (supplementary material 2.1).

Group Differences in Dynamic FNC Additionally Covarying for Mood Symptoms

Similarly, patterns of dysconnectivity were highly similar in the secondary analysis additionally covarying for mood symptoms. Only in state 3, additional hyperconnectivity within the CC domain was observed in PS youth compared to non-PS youth (supplementary material 2.2).

Dynamic Indices: Mean Dwell Time and Fraction of Time

Group was not included in either model. Age was negatively associated with the time spent, overall and before transitioning to another state, in states 1 (DMN-CC

Table 3. ICN-to-ICN Connectivity Pairs That Show Significant Group Effects in State 3 (DMN-CC-Antagonized State), Ordered by Domains

ICN1	ICN2	Domains	*P* value	*t*-value	Mean connectivity		Relationship
					Non-PS	PS	
Frontal pole L	Middle frontal gyrus R + L	CC-DMN	.00141	3.21	0.03	0.11	PS > non-PS
Superior frontal gyrus	Superior frontal gyrus medial	CC-DMN	.00014	–3.83	–0.13	–0.22	PS < non-PS
Temporal pole	Cerebellum R + L	limbic-CB	.00003	–4.21	0.04	–0.04	PS < non-PS
Temporal pole	Cerebellum R + L	limbic-CB	.00047	–3.52	0.04	–0.03	
Anterior insula R + L	SMA	SAL-SM	.00105	–3.30	0.07	–0.01	PS < non-PS
dACC	Posterior middle temporal gyrus R + L	SAL-VIS	.00148	3.20	–0.09	0.00	PS > non-PS
Insular cortex R + L	Posterior middle temporal gyrus R + L	SAL-VIS	.00111	3.28	–0.05	0.05	PS > non-PS
Putamen R + L	Superior frontal gyrus medial	SC-DMN	.00054	3.49	–0.09	–0.01	PS > non-PS
Putamen R + L	Postcentral gyrus L	SC-SM	.00101	–3.31	0.13	0.07	PS < non-PS
Putamen R+L	Postcentral gyrus L	SC-SM	.00073	–3.40	0.13	0.07	PS < non-PS
Putamen R + L	Paracentral lobule medial	SC-SM	.00119	–3.26	0.09	0.03	PS < non-PS
Putamen R + L	Precentral gyrus R + L	SC-SM	.00043	–3.55	0.12	0.06	PS < non-PS
Putamen R + L	SMA	SC-SM	.00125	–3.25	0.20	0.13	PS < non-PS
Ventral striatum	Fusiform gyrus R + L	SC-VIS	.00049	–3.51	0.07	–0.01	PS < non-PS
Postcentral gyrus L	Temporal pole	SM-limbic	.00079	3.38	–0.17	–0.10	PS > non-PS
Postcentral gyrus L	Posterior middle temporal gyrus R + L	SM-VIS	.00021	3.73	–0.01	0.09	PS > non-PS
Paracentral lobule medial	Posterior middle temporal Gyrus R + L	SM-VIS	.00113	3.28	0.02	0.09	PS > non-PS
Precentral gyrus R + L	Lingual gyrus R + L	SM-VIS	.00099	3.32	–0.03	0.05	PS > non-PS
Precentral gyrus R+L	Fusiform gyrus R + L	SM-VIS	.00007	4.02	–0.13	–0.05	PS > non-PS
Precentral gyrus R + L	Cuneus	SM-VIS	.00042	3.56	0.06	0.13	PS > non-PS
Precentral gyrus R + L	Posterior middle temporal Gyrus R + L	SM-VIS	.00077	3.38	–0.03	0.06	PS > non-PS
Supramarginal gyrus L	Posterior middle temporal gyrus R + L	SM-VIS	.00149	3.19	–0.01	0.09	PS > non-PS
SMA	Precuneus	SM-VIS	.00046	3.53	–0.29	–0.22	PS > non-PS
Supramarginal gyrus R + L	Posterior middle temporal gyrus R + L	SM-VIS	.00068	3.42	0.04	0.15	PS > non-PS
Cuneus	Frontal [ole L	VIS-CC	.00064	–3.44	–0.07	–0.15	PS < non-PS
Posterior middle temporal gyrus R + L	Superior parietal lobule R + L	VIS-CC	.00030	3.65	0.03	0.13	PS > non-PS
Fusiform gyrus R + L	rACC	VIS-DMN	.00037	–3.59	0.08	–0.01	PS < non-PS
Posterior middle temporal gyrus R + L	rACC	VIS-DMN	.00057	–3.47	0.07	–0.04	PS < non-PS
Posterior middle temporal gyrus R + L	Angular gyrus R + L	VIS-DMN	.00014	–3.84	0.09	–0.02	PS < non-PS
Posterior middle temporal gyrus R + L	Middle frontal gyrus R + L	VIS-DMN	.00037	–3.59	0.03	–0.07	PS < non-PS

Note: Abbreviations are explained in the first footnote to Table 2. AUD, auditory domain; dACC, dorsal anterior cingulate cortex

domain-synchronized state) and 5 (hypoconnected state): younger participants spent more time in these states. FT and MDT increased with age in states 3 (DMN-CC domain-antagonized state) and 4 (hyperconnected state with subcortical antagonism; supplementary material 2.2).

Discussion

We conducted the first investigation of whole-brain dynamic FNC in a young community sample experiencing PS relative to their peers. Results indicate several novel findings that distinctly advance our knowledge of functional dysconnectivity across the broader psychosis spectrum. First, PS-associated altered connectivity was primarily present in states characterized by synchronization or antagonism of the DMN and CC domains. We extend upon previous static functional connectivity findings of disruption of DMN-CC connectivity[10,56,57] by showing that the observed dysconnectivity is in fact state-dependent. Further, dysconnectivity in PS youth affects multiple brain networks; in addition to dysconnectivity of the DMN, CC, and salience domains in states 1 and 3, altered connectivity of sensorimotor and visual systems is pronounced in states 3, 4, and 5, completing the

Table 4. ICN-to-ICN Connectivity Pairs in State 4 (Hyperconnected State With Subcortical Antagonism) That Show Significant Group Effects and Group by Age Interaction Effects

	Significant group effects						
					Mean connectivity		
ICN1	ICN2	Domains	*P* value	t-value	Non-PS	PS	Relationship
Lingual gyrus R+L	Angular gyrus R	VIS-CC	.00024	3.72	–0.12	–0.11	PS > non-PS
Fusiform gyrus R+L	Angular gyrus R	VIS-CC	.0013	3.24	–0.13	–0.12	PS > non-PS
	Group by age interaction effects						
ICN1	ICN2	Domains	*P* value	*t*-value			
Lingual gyrus R+L	Angular gyrus R	VIS-CC	.0003	–3.7			
Posterior middle temporal Gyrus R+L	Inferior frontal gyrus L	AUD-CC	.001	3.3			

Note: Abbreviations are explained in the first footnote to Table 2.

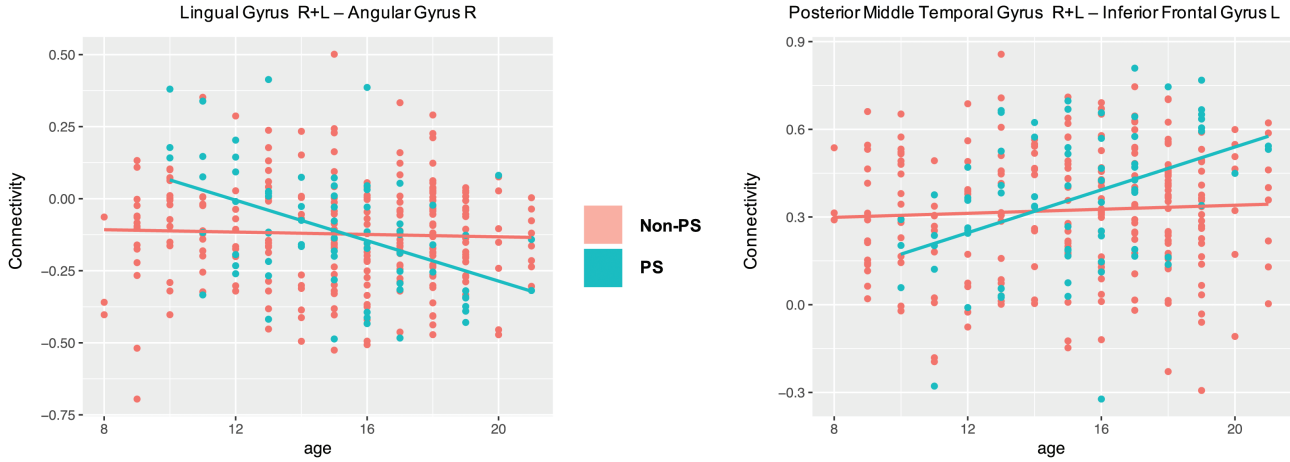

Fig. 4. Scatterplots of the significant group by age interaction in state 4.

picture of whole-brain dysconnectivity patterns associated with PS.

Psychosis Spectrum Criteria

The PS criteria we applied here are in accordance with previous reports on the PNC to facilitate comparisons across studies.[8,9,43,44,58] In contrast to CHR criteria applied in help-seeking populations,[59–61] criteria used here are broader, include negative and disorganized symptoms, and also consider age-appropriateness of symptoms.

Importantly, results of our secondary analyses of a continuous measure of symptom severity and additionally covarying for mood symptoms support findings from the primary analyses, revealing that most of the ICN pairs that significantly differed between PS youth and non-PS youth were also significantly associated with symptom severity and that patterns of dysconnectivity were robust when accounting for mood symptoms.

As such, these findings collectively suggest that the observed patterns of functional dysconnectivity become more extreme with increasing symptom severity and are relatively specific to PS symptoms (supplementary material 3).

Dynamic FNC

The most notable difference between whole-brain connectivity patterns of dynamic states across groups is that state 1 is accompanied by positive connectivity between the DMN and the CC domain, whereas state 3 shows antagonism between DMN and CC, salience, and sensorimotor domains. Changes in connectivity between DMN and CC domains are important for adapting to cognitive demands,[62,63] and the anterior insula, a major component of the salience domain, has been suggested to modulate connectivity between these domains.[64,65] States 1 and 3 therefore capture snapshots of changing connectivity between the DMN and the CC domains; prominence of dysconnectivity in these states may indicate that disruption of these functional domains is particularly implicated in the emergence of PS.

Table 5. ICN-to-ICN Connectivity Pairs in State 5 (Hypoconnected State) That Show Significant Group Effects

ICN1	ICN2	Domains	*P* value	*t*-value	Mean connectivity		Relationship
					Non-PS	PS	
Superior parietal lobule R+L	Cerebellum	CC-CB	.00022	–3.73	0.02	–0.03	PS < non-PS
Inferior parietal lobule L	Cerebellum R + L	CC-CB	.00113	3.28	–0.03	0.08	PS > non-PS
rACC	Cerebellum	DMN-CB	.00064	–3.44	–0.05	–0.10	PS < non-PS
Putamen R+L	Lingual gyrus R + L	SC-VIS	.00094	3.33	–0.06	–0.04	PS > non-PS
Lingual gyrus R+L	Cerebellum	VIS-CB	.00127	–3.24	0.34	0.33	PS < non-PS
Lateral inferior occipital gyrus R + L	Cerebellum	VIS-CB	.00122	–3.25	0.37	0.34	PS < non-PS
Cuneus	Cerebellum	VIS-CB	.00003	–4.25	0.39	0.37	PS < non-PS
Inferior occipital gyrus R + L	Cerebellum	VIS-CB	.00103	–3.30	0.28	0.24	PS < non-PS
Inferior occipital gyrus R + L	Cerebellum	VIS-CB	.00129	–3.24	0.40	0.35	PS < non-PS
Fusiform gyrus R + L	Inferior parietal lobule	VIS-CC	.00097	3.32	0.12	0.15	PS > non-PS
Fusiform gyrus R + L	Middle frontal gyrus R + L	VIS-CC	.00002	4.33	0.00	0.06	PS > non-PS
Fusiform gyrus R + L	Frontal pole L	VIS-CC	.00102	3.30	0.04	0.09	PS > non-PS
Lateral inferior occipital gyrus R + L	Middle frontal gyrus R + L	VIS-CC	.00020	3.76	–0.14	–0.06	PS > non-PS
Lateral inferior occipital gyrus R + L	Angular gyrus R	VIS-CC	.00082	3.37	–0.17	–0.14	PS > non-PS
Inferior occipital gyrus R + L	Inferior frontal gyrus R	VIS-CC	.00060	3.45	–0.03	0.02	PS > non-PS
Inferior occipital gyrus R + L	Superior parietal lobule R + L	VIS-CC	.00048	–3.52	–0.05	–0.10	PS < non-PS
Inferior occipital gyrus R + L	Superior parietal lobule	VIS-CC	.00064	–3.44	0.05	0.03	PS < non-PS
Lateral inferior occipital gyrus R + L	Angular gyrus R + L	VIS-DMN	.00028	3.66	–0.09	–0.03	PS > non-PS
Lingual gyrus R + L	Lateral inferior occipital gyrus R + L	VIS-VIS	.00037	–3.59	0.16	0.10	PS < non-PS
Lingual gyrus R + L	Inferior occipital gyrus R + L	VIS-VIS	.00031	–3.63	0.08	0.00	PS < non-PS
Lingual gyrus R + L	Inferior occipital gyrus R + L	VIS-VIS	.00073	–3.40	0.14	0.08	PS < non-PS
Lateral inferior occipital gyrus R + L	Cuneus	VIS-VIS	.00035	–3.60	0.27	0.20	PS < non-PS
Lateral inferior occipital gyrus R + L	Inferior occipital gyrus R + L	VIS-VIS	.00136	–3.22	0.37	0.33	PS < non-PS
Cuneus	Inferior occipital gyrus R + L	VIS-VIS	.00013	–3.85	0.16	0.10	PS < non-PS
Cuneus	Inferior occipital gyrus R + L	VIS-VIS	.00005	–4.08	0.18	0.13	PS < non-PS

Note: Abbreviations are explained in the first footnote to Table 2.

By applying multivariate model selection, we found that different sets of covariates were selected for each dynamic state, indicating that group, sex, age, and maternal education have differential contributions to the variance of FNC across different states. The group variable was included in all but one model, and most of the differences between PS and non-PS youth occurred in states 1 and 3.

Developmental rs-fMRI studies of static FNC have shown that connectivity between DMN and CC domains decreases with age, whereas connectivity *within* these domains increases with age;[66–68] In line with these findings of age-associated decreases of DMN-CC connectivity, we found that MDT and FT of state 3 (DMN-CC domain-antagonized state) increased with age, whereas MDT and FT of state 1 (DMN-CC domain-synchronized state) decreased with age: older participants tend to spend more time in states exhibiting antagonism between DMN and CC domains and less time in states characterized by synchronization of these domains.

Overall, our results expand upon recent findings of state-dependent dysconnectivity identified in adults with schizophrenia and those at risk for developing psychosis, by revealing qualitatively similar patterns of dynamic dysconnectivity. In addition, we find that dysconnectivity in dynamic FNC in youth experiencing PS is most pronounced in sensorimotor and visual areas, warranting further prospective longitudinal investigations of the involvement of these domains in developmental trajectories of PS.

State 1: The DMN-CC Domain-Synchronized State.
In state 1, PS youth exhibited dysconnectivity of prefrontal brain areas assigned to the salience and DMN domains relative to non-PS participants. In a recent investigation of the association between static FNC and dimensions of psychopathology in this cohort, PS were associated with increased connectivity between the DMN and CC domains.[10] Further, a recent study of dynamic FNC in a CHR cohort found less temporal

variability of functional connectivity in regions of the DMN and salience domains relative to healthy controls.[69] PS-associated dysconnectivity between DMN and salience domains[56,65,70–72] may be a neural underpinning of the aberrant salience theory of schizophrenia;[73,74] this theory posits that internal and external stimuli that are competing for "attention" are falsely categorized as salient, ultimately leading to PS.[71] The anterior insula not only detects salient stimuli but also orchestrates connectivity between the DMN and CC domain in response to those stimuli.[64,71]

We also found that, in this state, PS youth showed long-range hypoconnectivity between prefrontal CC areas and the cerebellum. Interestingly, prior studies in healthy adults have associated stronger prefrontal-cerebellar connectivity with better executive functioning.[75]

PS youth also exhibited hypoconnectivity in state 1 between the basal ganglia and the sensorimotor domain relative to non-PS youth. Subcortical-cortical dysconnectivity has been used in the psychosis spectrum.[36,76,77] Recent findings suggest an association between disruption of the cortico-basal ganglia loop and motor impairments in patients with schizophrenia.[78–80] Behavioral data indicate that abnormal involuntary movements are linked to psychosis risk in youth,[81] and cortical-subcortical dysconnectivity may be a contributing factor.

State 3: DMN-CC Domain-Antagonized State.
State 3 was the most common state in both groups. Here, dysconnectivity in PS participants primarily involved visual and sensorimotor domains. A substantial body of literature indicates alterations in visual processing in schizophrenia.[82–85] Moreover, behavioral studies in the offspring of patients with psychotic disorders indicate an association between early visual abnormalities and later development of psychosis.[86,87] Aberrant functional connectivity of the visual domain—which we observed across multiple states—might underlie these early perceptual processing impairments associated with PS.

The visual domain showed notable group by age interaction effects in state 4: connectivity between visual association areas and the angular gyrus showed age-associated decreases in PS youth, but not in non-PS youth. In contrast, connectivity between auditory association cortices and the inferior frontal gyrus increased in PS youth with age which, again, was not observed in non-PS youth. In accordance with these findings, it has been shown that multisensory integration, a function of association cortices, is disrupted in patients with schizophrenia.[88,89]

In summary, our findings of dysconnectivity involving multisensory association cortices could map onto the hypothesis that multisensory integration deficits are indeed among the earliest impairments along with the psychosis spectrum.[7]

Dynamic Indices

Contrary to our hypotheses, there were no group differences for MDT or FT, suggesting that changes in these global metrics may only be detectable at the severe end of the psychosis continuum.[33,36] This notion is supported by previous studies; whereas patients with schizophrenia spent significantly more time in hypoconnected states relative to healthy controls,[36] CHR individuals did not differ from healthy controls in MDT/FT.[33] However, given recent findings that adults endorsing psychotic-like experiences have significantly longer MDT in hypoconnected states,[35] the lack of a difference in our study could also be due to developmental effects; ie, potential MDT differences in PS youth may be overlaid by developmental changes in MDT.

Limitations

Even though PS youth have an increased risk for developing overt psychosis,[1,4] most of them will not develop a psychotic disorder. Longitudinal studies will be essential to understand symptom development and progression, and factors contributing to heterogeneity in outcome. Finally, longer rs-fMRI scans may allow more stable FNC estimations.[53,90–92] See supplementary material 4.

Conclusion

This study provides new evidence that disruptions of dynamic FNC are present even at the less severe end of the psychosis continuum, complementing previous work on help-seeking and clinically diagnosed cohorts representing the more severe end of this spectrum.

Taken together, dysconnectivity observed in states 1 and 3 highlights networks previously associated with cognitive impairment in individuals on the psychosis spectrum,[9,10] whereas alterations in other transient states reveal abnormal connectivity in the visual and sensorimotor system. Metrics of dynamic FNC offer promise as future diagnostic or prognostic indicators and potential targets for therapeutic interventions.[27,36,93–97]

Supplementary Material

Supplementary data are available at *Schizophrenia Bulletin* online

Funding

Research was supported by National Institute of Mental Health grants R01 MH107250 (CEB, RAO), R01 MH101506 (KHK), K01 MH112774 (MJ), and K99 MH116115 (LMOL).

Acknowledgment

Data were downloaded from dbGaP (phs000607.v1.p1, C. E. Bearden, #7147). The authors have declared that

there are no conflicts of interest in relation to the subject of this study

References

1. David AS, Ajnakina O. Psychosis as a continuous phenotype in the general population: the thin line between normality and pathology. *World Psychiatry*. 2016;15(2):129–130.
2. DeRosse P, Karlsgodt KH. Examining the psychosis continuum. *Curr Behav Neurosci Rep*. 2015;2(2):80–89.
3. Guloksuz S, van Os J. The slow death of the concept of schizophrenia and the painful birth of the psychosis spectrum. *Psychol Med*. 2018;48(2):229–244.
4. Poulton R, Caspi A, Moffitt TE, Cannon M, Murray R, Harrington H. Children's self-reported psychotic symptoms and adult schizophreniform disorder: a 15-year longitudinal study. *Arch Gen Psychiatry*. 2000;57(11):1053–1058.
5. Linscott RJ, van Os J. An updated and conservative systematic review and meta-analysis of epidemiological evidence on psychotic experiences in children and adults: on the pathway from proneness to persistence to dimensional expression across mental disorders. *Psychol Med*. 2013;43(6):1133–1149.
6. Cannon TD. How schizophrenia develops: cognitive and brain mechanisms underlying onset of psychosis. *Trends Cogn Sci*. 2015;19(12):744–756.
7. Forsyth JK, Lewis DA. Mapping the consequences of impaired synaptic plasticity in schizophrenia through development: an integrative model for diverse clinical features. *Trends Cogn Sci*. 2017;21(10):760–778.
8. Gur RC, Calkins ME, Satterthwaite TD, et al. Neurocognitive growth charting in psychosis spectrum youths. *JAMA Psychiatry*. 2014;71(4):366–374.
9. Satterthwaite TD, Vandekar SN, Wolf DH, et al. Connectome-wide network analysis of youth with psychosis-spectrum symptoms. *Mol Psychiatry*. 2015;20(12):1508–1515.
10. Xia CH, Ma Z, Ciric R, et al. Linked dimensions of psychopathology and connectivity in functional brain networks. *Nat Commun*. 2018;9(1):3003.
11. Gogtay N, Giedd JN, Lusk L, et al. Dynamic mapping of human cortical development during childhood through early adulthood. *Proc Natl Acad Sci USA*. 2004;101(21):8174–8179.
12. Giedd JN, Blumenthal J, Jeffries NO, et al. Brain development during childhood and adolescence: a longitudinal MRI study. *Nat Neurosci*. 1999;2(10):861–863.
13. Mills KL, Goddings AL, Clasen LS, Giedd JN, Blakemore SJ. The developmental mismatch in structural brain maturation during adolescence. *Dev Neurosci*. 2014;36(3–4):147–160.
14. Laurens KR, Hobbs MJ, Sunderland M, Green MJ, Mould GL. Psychotic-like experiences in a community sample of 8000 children aged 9 to 11 years: an item response theory analysis. *Psychol Med*. 2012;42(7):1495–1506.
15. Keshavan MS, Giedd J, Lau JY, Lewis DA, Paus T. Changes in the adolescent brain and the pathophysiology of psychotic disorders. *Lancet Psychiatry*. 2014;1(7):549–558.
16. Paus T, Keshavan M, Giedd JN. Why do many psychiatric disorders emerge during adolescence? *Nat Rev Neurosci*. 2008;9(12):947–957.
17. Calhoun VD, Eichele T, Pearlson G. Functional brain networks in schizophrenia: a review. *Front Hum Neurosci*. 2009;3:17.
18. Friston K, Brown HR, Siemerkus J, Stephan KE. The dysconnection hypothesis (2016). *Schizophr Res*. 2016;176(2-3):83–94.
19. Fornito A, Zalesky A, Pantelis C, Bullmore ET. Schizophrenia, neuroimaging and connectomics. *Neuroimage*. 2012;62(4):2296–2314.
20. Biswal B, Yetkin FZ, Haughton VM, Hyde JS. Functional connectivity in the motor cortex of resting human brain using echo-planar MRI. *Magn Reson Med*. 1995;34(4):537–541.
21. Fox MD, Raichle ME. Spontaneous fluctuations in brain activity observed with functional magnetic resonance imaging. *Nat Rev Neurosci*. 2007;8(9):700–711.
22. Friston KJ. Functional and effective connectivity: a review. *Brain Connect*. 2011;1(1):13–36.
23. Chang C, Glover GH. Time-frequency dynamics of resting-state brain connectivity measured with fMRI. *Neuroimage*. 2010;50(1):81–98.
24. Hutchison RM, Womelsdorf T, Gati JS, Everling S, Menon RS. Resting-state networks show dynamic functional connectivity in awake humans and anesthetized macaques. *Hum Brain Mapp*. 2013;34(9):2154–2177.
25. Hutchison RM, Morton JB. Tracking the brain's functional coupling dynamics over development. *J Neurosci*. 2015;35(17):6849–6859.
26. Matsui T, Murakami T, Ohki K. Neuronal origin of the temporal dynamics of spontaneous BOLD activity correlation. *Cereb Cortex*. 2018;29(4):1496–1508.
27. Hutchison RM, Womelsdorf T, Allen EA, et al. Dynamic functional connectivity: promise, issues, and interpretations. *Neuroimage*. 2013;80:360–378.
28. Satterthwaite TD, Baker JT. How can studies of resting-state functional connectivity help us understand psychosis as a disorder of brain development? *Curr Opin Neurobiol*. 2015;30:85–91.
29. Allen EA, Damaraju E, Plis SM, Erhardt EB, Eichele T, Calhoun VD. Tracking whole-brain connectivity dynamics in the resting state. *Cereb Cortex*. 2014;24(3):663–676.
30. Chen JE, Chang C, Greicius MD, Glover GH. Introducing co-activation pattern metrics to quantify spontaneous brain network dynamics. *Neuroimage*. 2015;111:476–488.
31. Lindquist MA, Xu Y, Nebel MB, Caffo BS. Evaluating dynamic bivariate correlations in resting-state fMRI: a comparison study and a new approach. *Neuroimage*. 2014;101:531–546.
32. Yu Q, Erhardt EB, Sui J, et al. Assessing dynamic brain graphs of time-varying connectivity in fMRI data: application to healthy controls and patients with schizophrenia. *Neuroimage*. 2015;107:345–355.
33. Mennigen E, Fryer SL, Rashid B, et al. Transient patterns of functional dysconnectivity in clinical high risk and early illness schizophrenia individuals compared with healthy controls. *Brain Connect*. 2019;9(1):60–76.
34. Du Y, Fryer SL, Fu Z, et al. Dynamic functional connectivity impairments in early schizophrenia and clinical high-risk for psychosis. *Neuroimage*. 2018;180(Pt B):632–645.
35. Barber AD, Lindquist MA, DeRosse P, Karlsgodt KH. Dynamic functional connectivity states reflecting psychotic-like experiences. *Biol Psychiatry Cogn Neurosci Neuroimaging*. 2018;3(5):443–453.
36. Damaraju E, Allen EA, Belger A, et al. Dynamic functional connectivity analysis reveals transient states of dysconnectivity in schizophrenia. *Neuroimage Clin*. 2014;5:298–308.

37. Du Y, Pearlson GD, Yu Q, et al. Interaction among subsystems within default mode network diminished in schizophrenia patients: a dynamic connectivity approach. *Schizophr Res*. 2016;170(1):55–65.
38. Kaufman J, Birmaher B, Brent D, et al. Schedule for affective disorders and schizophrenia for school-age children-present and lifetime version (K-SADS-PL): initial reliability and validity data. *J Am Acad Child Adolesc Psychiatry*.. 1997;36(7):980–988. doi:10.1097/00004583-199707000-00021
39. Calkins ME, Merikangas KR, Moore TM, et al. The Philadelphia Neurodevelopmental Cohort: constructing a deep phenotyping collaborative. *J Child Psychol Psychiatry*. 2015;56(12):1356–1369.
40. Gur RC, Richard J, Hughett P, et al. A cognitive neuroscience-based computerized battery for efficient measurement of individual differences: standardization and initial construct validation. *J Neurosci Methods*. 2010;187(2):254–262.
41. Satterthwaite TD, Elliott MA, Ruparel K, et al. Neuroimaging of the Philadelphia neurodevelopmental cohort. *Neuroimage*. 2014;86:544–553.
42. Kessler D, Angstadt M, Sripada C. Growth charting of brain connectivity networks and the identification of attention impairment in youth. *JAMA Psychiatry*. 2016;73(5):481–489.
43. Calkins ME, Moore TM, Merikangas KR, et al. The psychosis spectrum in a young U.S. community sample: findings from the Philadelphia Neurodevelopmental Cohort. *World Psychiatry*. 2014;13(3):296–305.
44. Wolf DH, Satterthwaite TD, Calkins ME, et al. Functional neuroimaging abnormalities in youth with psychosis spectrum symptoms. *JAMA Psychiatry*. 2015;72(5):456–465.
45. Roalf DR, Quarmley M, Calkins ME, et al. Temporal lobe volume decrements in psychosis spectrum youths. *Schizophr Bull*. 2017;43(3):601–610. doi:10.1093/schbul/sbw112
46. Satterthwaite TD, Wolf DH, Calkins ME, et al. Structural brain abnormalities in youth with psychosis spectrum symptoms. *JAMA Psychiatry*. 2016;73(5):515–524.
47. Kobayashi H, Nemoto T, Koshikawa H, et al. A self-reported instrument for prodromal symptoms of psychosis: testing the clinical validity of the PRIME Screen-Revised (PS-R) in a Japanese population. *Schizophr Res*. 2008;106(2-3):356–362.
48. Merikangas KR, Avenevoli S, Costello EJ, Koretz D, Kessler RC. National comorbidity survey replication adolescent supplement (NCS-A): I. Background and measures. *J Am Acad Child Adolesc Psychiatry*.. 2009;48(4):367–379. doi:10.1097/CHI.0b013e31819996f1
49. McGlashan TH, Miller TJ, Woods SW, Hoffman RE, Davidson L. Instrument for the assessment of prodromal symptoms and states. In: Miller T, Mednick SA, McGlashan TH, Libiger J, Johannessen JO, eds. *Early Intervention in Psychotic Disorders. NATO Science Series*. the Netherlands: Springer; 2001:135–149. doi:10.1007/978-94-010-0892-1_7
50. Calhoun VD, Adali T, Pearlson GD, Pekar JJ. A method for making group inferences from functional MRI data using independent component analysis. *Hum Brain Mapp*. 2001;14(3):140–151.
51. Allen EA, Erhardt EB, Damaraju E,et al. A baseline for the multivariate comparison of resting-state networks. *Front Syst Neurosci*. 2011;5:2.
52. Tzourio-Mazoyer N, Landeau B, Papathanassiou D, et al. Automated anatomical labeling of activations in SPM using a macroscopic anatomical parcellation of the MNI MRI single-subject brain. *Neuroimage*. 2002;15(1):273–289. doi:10.1006/nimg.2001.0978
53. Yarkoni T. Neurosynth. http://neurosynth.org/. Accessed August 16, 2016.
54. Abrol A, Damaraju E, Miller RL, et al. Replicability of time-varying connectivity patterns in large resting state fMRI samples. *Neuroimage*. 2017;163:160–176.
55. Tooley UA, Mackey AP, Ciric R, et al. Influence of Neighborhood SES on Functional Brain Network Development. arXiv preprint. *arXiv*:1807.07687.
56. Wotruba D, Michels L, Buechler R, et al. Aberrant coupling within and across the default mode, task-positive, and salience network in subjects at risk for psychosis. *Schizophr Bull*. 2014;40:1095–1104. doi:10.1093/schbul/sbt161
57. Tang J, Liao Y, Song M, et al. Aberrant default mode functional connectivity in early onset schizophrenia. *PLoS One*. 2013;8(7):e71061. doi:10.1371/journal.pone.0071061
58. Calkins ME, Moore TM, Satterthwaite TD, et al. Persistence of psychosis spectrum symptoms in the Philadelphia Neurodevelopmental Cohort: a prospective two-year follow-up. *World Psychiatry*. 2017;16(1):62–76.
59. Addington J, Liu L, Buchy L, et al. North American Prodrome Longitudinal Study (NAPLS 2): the prodromal symptoms. *J Nerv Ment Dis*. 2015;203(5):328–335.
60. Addington J, Cadenhead KS, Cornblatt BA, et al. North American Prodrome Longitudinal Study (NAPLS 2): overview and recruitment. *Schizophr Res*. 2012;142(1–3):77–82.
61. McGlashan T, Walsh B, Woods S. *The Psychosis-Risk Syndrome: Handbook for Diagnosis and Follow-Up*. USA: Oxford University Press; 2010.
62. Shine JM, Bissett PG, Bell PT, et al. The dynamics of functional brain networks: integrated network states during cognitive task performance. *Neuron*. 2016;92(2):544–554.
63. Vatansever D, Menon DK, Manktelow AE, Sahakian BJ, Stamatakis EA. Default mode dynamics for global functional integration. *J Neurosci*. 2015;35(46):15254–15262.
64. Menon V, Uddin LQ. Saliency, switching, attention and control: a network model of insula function. *Brain Struct Funct*. 2010;214(5–6):655–667.
65. Goulden N, Khusnulina A, Davis NJ, et al. The salience network is responsible for switching between the default mode network and the central executive network: replication from DCM. *Neuroimage*. 2014;99:180–190.
66. Sherman LE, Rudie JD, Pfeifer JH, Masten CL, McNealy K, Dapretto M. Development of the default mode and central executive networks across early adolescence: a longitudinal study. *Dev Cogn Neurosci*. 2014;10:148–159.
67. Mak LE, Minuzzi L, MacQueen G, Hall G, Kennedy SH, Milev R. The default mode network in healthy individuals: a systematic review and meta-analysis. *Brain Connect*. 2016;7(1):25–33. doi:10.1089/brain.2016.0438
68. Marusak HA, Calhoun VD, Brown S, et al. Dynamic functional connectivity of neurocognitive networks in children. *Hum Brain Mapp*. 2017;38(1):97–108.
69. Pelletier-Baldelli A, Andrews-Hanna JR, Mittal VA. Resting state connectivity dynamics in individuals at risk for psychosis. *J Abnorm Psychol*. 2018;127(3):314–325. doi:10.1037/abn0000330
70. Manoliu A, Riedl V, Zherdin A, et al. Aberrant dependence of default mode/central executive network interactions on anterior insular salience network activity in schizophrenia. *Schizophr Bull*. 2014;40(2):428–437.
71. Uddin LQ. Salience processing and insular cortical function and dysfunction. *Nat Rev Neurosci*. 2015;16(1):55–61.

72. Palaniyappan L, Simmonite M, White TP, Liddle EB, Liddle PF. Neural primacy of the salience processing system in schizophrenia. *Neuron*. 2013;79(4):814–828.
73. Palaniyappan L, Liddle PF. Does the salience network play a cardinal role in psychosis? An emerging hypothesis of insular dysfunction. *J Psychiatry Neurosci*. 2012;37(1):17–27. doi:10.1503/jpn.100176
74. Kapur S. Psychosis as a state of aberrant salience: a framework linking biology, phenomenology, and pharmacology in schizophrenia. *Am J Psychiatry*. 2003;160(1):13–23. http://ajp.psychiatryonline.org/doi/pdf/10.1176/appi.ajp.160.1.13. Accessed May 2, 2016.
75. Reineberg AE, Andrews-Hanna JR, Depue BE, Friedman NP, Banich MT. Resting-state networks predict individual differences in common and specific aspects of executive function. *Neuroimage*. 2015;104:69–78.
76. Anticevic A, Haut K, Murray JD, et al. Association of thalamic dysconnectivity and conversion to psychosis in youth and young adults at elevated clinical risk. *JAMA Psychiatry*. 2015;72(9):882–891.
77. Ferri J, Fryer SL, Roach BJ, Loewy RL, Ford JM, Mathalon DH. Thalamic dysconnectivity in individuals at clinically high risk for schizophrenia and during early illness. *Schizophr Bull*.. 2017;43(suppl_1):S44–S44. doi:10.1093/schbul/sbx021.116),
78. Skåtun KC, Kaufmann T, Doan NT, et al.; KaSP. Consistent functional connectivity alterations in schizophrenia spectrum disorder: a multisite study. *Schizophr Bull*. 2017;43(4):914–924.
79. Bracht T, Schnell S, Federspiel A, et al. Altered cortico-basal ganglia motor pathways reflect reduced volitional motor activity in schizophrenia. *Schizophr Res*. 2013;143(2-3):269–276.
80. Walther S. Psychomotor symptoms of schizophrenia map on the cerebral motor circuit. *Psychiatry Res*. 2015;233(3):293–298.
81. Kindler J, Schultze-Lutter F, Michel C, et al. Abnormal involuntary movements are linked to psychosis-risk in children and adolescents: results of a population-based study. *Schizophr Res*. 2016;174(1–3):58–64.
82. Chen Y. Abnormal visual motion processing in schizophrenia: a review of research progress. *Schizophr Bull*. 2011;37(4):709–715.
83. Silverstein SM, Keane BP. Perceptual organization impairment in schizophrenia and associated brain mechanisms: review of research from 2005 to 2010. *Schizophr Bull*. 2011;37(4):690–699. doi:10.1093/schbul/sbr052
84. Butler PD, Silverstein SM, Dakin SC. Visual perception and its impairment in schizophrenia. *Biol Psychiatry*. 2008;64(1):40–47.
85. Silverstein S, Keane BP, Blake R, Giersch A, Green M, Kéri S. Vision in schizophrenia: why it matters. *Front Psychol*. 2015;6:41.
86. Schubert EW, Henriksson KM, McNeil TF. A prospective study of offspring of women with psychosis: visual dysfunction in early childhood predicts schizophrenia-spectrum disorders in adulthood. *Acta Psychiatr Scand*. 2005;112(5):385–393.
87. Schiffman J, Maeda JA, Hayashi K, et al. Premorbid childhood ocular alignment abnormalities and adult schizophrenia-spectrum disorder. *Schizophr Res*. 2006;81(2-3):253–260.
88. Stevenson RA, Park S, Cochran C, et al. The associations between multisensory temporal processing and symptoms of schizophrenia. *Schizophr Res*. 2017;179:97–103.
89. Tseng HH, Bossong MG, Modinos G, Chen KM, McGuire P, Allen P. A systematic review of multisensory cognitive-affective integration in schizophrenia. *Neurosci Biobehav Rev*. 2015;55:444–452.
90. Hindriks R, Adhikari MH, Murayama Y, et al. Can sliding-window correlations reveal dynamic functional connectivity in resting-state fMRI? *Neuroimage*. 2016;127:242–256.
91. Preti MG, Bolton TA, Van De Ville D. The dynamic functional connectome: state-of-the-art and perspectives. *Neuroimage*. 2017;160:41–54.
92. Miller RL, Abrol A, Adali T, Levin-Schwarz Y, Calhoun VD. Resting-state fMRI dynamics and null models: Perspectives, sampling variability, and simulations. *Front neurosci*. 2018;12. June 2017:153411. doi:10.1101/153411
93. Rashid B, Arbabshirani MR, Damaraju E, et al. Classification of schizophrenia and bipolar patients using static and dynamic resting-state fMRI brain connectivity. *Neuroimage*. 2016;134:645–657.
94. Kaiser RH, Whitfield-Gabrieli S, Dillon DG, et al. Dynamic resting-state functional connectivity in major depression. *Neuropsychopharmacology*. 2016;41(7):1822–1830.
95. de Lacy N, Calhoun VD. Dynamic connectivity and the effects of maturation in youth with attention deficit hyperactivity disorder. *Netw Neurosci*. 2018:1–41. doi:10.1162/netn_a_00063
96. de Lacy N, Doherty D, King BH, Rachakonda S, Calhoun VD. Disruption to control network function correlates with altered dynamic connectivity in the wider autism spectrum. *Neuroimage Clin*. 2017;15:513–524.
97. Rashid B, Damaraju E, Pearlson GD, Calhoun VD. Dynamic connectivity states estimated from resting fMRI Identify differences among Schizophrenia, bipolar disorder, and healthy control subjects. *Front Hum Neurosci*. 2014;8:897. http://www.ncbi.nlm.nih.gov/pmc/articles/PMC4224100/.